Journal of Power Sources 182 (2008) 119–123

Contents lists available at ScienceDirect

Journal of Power Sources

journal homepage: www.elsevier.com/locate/jpowsour

Short communication

Improvement in dye-sensitized solar cells employing TiO_2 electrodes coated with Al_2O_3 by reactive direct current magnetron sputtering

Sujuan Wu, Hongwei Han, Qidong Tai, Jing Zhang, Sheng Xu, Conghua Zhou, Ying Yang, Hao Hu, BoLei Chen, Xing-zhong Zhao*

Department of Electronical Science and Technology, School of Physical Science and Technology, Key Laboratory of Acoustic and Photonic Materials and Devices of Ministry of Education, Wuhan University, Wuhan 430072, PR China

ARTICLE INFO

Article history:
Received 7 November 2007
Received in revised form 18 March 2008
Accepted 23 March 2008
Available online 29 March 2008

Keywords:
Reactive dc magnetron sputtering
O_2 plasma
Al_2O_3-coated TiO_2 electrodes
Dye-sensitized TiO_2 solar cells
Performance

ABSTRACT

A novel surface modification method was carried out by reactive dc magnetron sputtering to fabricate TiO_2 electrodes coated with Al_2O_3 for improving the performance of dye-sensitized solar cells (DSSCs). The Al_2O_3-coated TiO_2 electrodes had been characterized by X-ray photoelectron spectroscopy (XPS), scanning electron microscopy (SEM), UV–vis spectrophotometer, cyclic voltammetry (CV), and electrochemical impedance spectroscopy (EIS). The study results revealed that the modification to TiO_2 increases dye absorption amount, reduces trap sites on TiO_2, and suppresses interfacial recombination. The impact of sputtering time on photoelectric performance of DSSCs was investigated. Sputtering Al_2O_3 for 4 min on 5-μm thick TiO_2 greatly improves all cell parameters, resulting in enhancing the conversion efficiency from 3.93% to 5.91%. Further increasing sputtering time decreases conversion efficiency.

1. Introduction

Dye-sensitized solar cells (DSSCs) have been regarded as one of the most promising candidates to replace silicon cells since O'Regan et al. reported their breakthrough results in 1991 [1]. As the key component of DSSCs, the nanoporous electrode shows high surface area, which enables both efficient electron injection and light harvesting. Unfortunately, the nanoporous electrode also introduces the charge recombination which mainly occurs at the electrode/electrolyte interface due to the absence of energy barrier layer [2,3]. In the last decade, several methods have been applied to reduce recombination at the interface including dip-coating in a solution to fabricate an insulating layer on TiO_2 [3–10], spin-coating a solution on TiO_2 followed by oxidation [11,12], chemical vapor deposition [13], electrochemical deposition [14,15], and mixing of metal salts such as $Al(NO_3)_3$ and $AlCl_3$ with TiO_2 or SnO_2 nanoparticles in solution [16,17]. However, most of the modifications are chemical methods. To make DSSCs a commercially competitive technology, a recombination barrier layer prepared by easily available method is needed in DSSCs.

Han et al. reported that the TiO_2 electrode treated with Ar plasma shows better reactive activity [18]. Recently, Kim et al. found that treating TiO_2 with O_2 plasma can reduce oxygen vacancies on TiO_2, increase dye absorption, and improve performance of DSSCs [19,20]. It was reported that exposing TiO_2 to an O_2 atmosphere can reduce oxygen vacancies on TiO_2 [21–23]. Aronsson et al. reported that treating TiO_2 film by O_2 plasma can produce a uniform and stoichiometric surface layer on TiO_2 [24]. Gan et al. demonstrated that O_2 plasma treatment has an effect on the surface cleanness and the stoichiometry of TiO_2 (1 1 0) [25]. These indicated that using Ar or O_2 plasma to treat TiO_2 films is a feasible method to enhance the efficiency of DSSCs. Yanagida et al. found that the deposition of Nb_2O_5 on conducting glass by RF magnetron sputtering significantly improve the performance of dye-sensitized ionic liquid solar cells [26,27]. Their reports present that the method of magnetron sputtering can be used to deposit barrier layer in DSSCs.

In DSSCs, oxygen vacancies on TiO_2 surfaces can be easily produced during the annealing of TiO_2 films. However, the efficiency and photocurrent decreases with the abundance of oxygen vacancies, since these oxygen vacancies on TiO_2 surfaces provide electron traps and thus prevent electron transport in the system. To improve the efficiency of DSSCs, we must reduce oxygen vacancies and increase dye absorption amount. In the process of the sputtering, the Ar plasma can enhance reactive activity while the O_2 plasma can decrease oxygen vacancies and create a hydrophilic surface to facilitate dye absorption. Moreover, as an electric-insulating oxide, the conduction band edge of Al_2O_3 is significantly negative of both the TiO_2 conduction band edge and dye excited state

* Corresponding author. Tel.: +86 27 87642784; fax: +86 27 68752569.
E-mail address: xzzhao@whu.edu.cn (X.-z. Zhao).

0378-7753/$ – see front matter.
doi:10.1016/j.jpowsour.2008.03.054

oxidation potential, indicating that Al_2O_3 can function as physical barrier layer for both electron injection and charge electron recombination reactions [9]. Furthermore, the higher isoelectric point (iep) of Al_2O_3 (iep at pH 9) compared to anatase TiO_2 (iep at pH 6.2) favors stronger dye adsorption and thus better light absorption [16]. On the basis of these considerations, we fabricated DSSCs based on TiO_2 electrodes coated with Al_2O_3 (TiO_2/Al_2O_3) prepared by reactive dc magnetron sputtering, and investigated the effects of sputtering Al_2O_3 for different time on micrograph, the absorption and transmission properties, dye adsorption amount, surface states on TiO_2, interfacial electrochemical characteristic, and performance of the DSSC.

2. Experimental

2.1. Materials

All the regents used were of analytical purity. $LiClO_4$, 2-propanol, Triton-X100, poly(ethylene glycol) (PEG, MW = 20,000) and propylene carbonate (PC) were purchased from Sinopharm Chemical Reagent Corporation (China). I_2 was obtained from Beijing Yili chemicals (China). LiI, titanium tetraisopropoxide and 4-*tert*-butylpyridine were obtained from Acros. The Ru dye, N719 (Ruthenium 535 bis-TBA) and 1,2-dimethyl-3-*n*-propylimidazolium was purchased from Solaronix (Switzerland). Fluorine-doped SnO_2 conductive glass (FTO, transmission >80% in the visible, sheet resistance 20 $\Omega\,sq^{-1}$) obtained from China Yaohua Glass Group Corporation was used as the substrate to deposit TiO_2 films. The metal aluminum target (purity 99.9%) was purchased from Beijing Cuibolin Non-ferrous Technology Developing Co., Ltd.

2.2. Preparation of TiO_2/Al_2O_3

Anatase TiO_2 colloids were prepared by hydrolysis of titanium tetraisopropoxide. The TiO_2 slurry was spread on FTO by a glass rod, using adhesive tapes as spacers. After the TiO_2 films dried, they were sintered in air. The thickness of TiO_2 films was about 5 μm, controlled using tapes. The Al_2O_3 was deposited on TiO_2 by reactive direct current magnetron sputtering to fabricate TiO_2/Al_2O_3 electrodes. The sputtering target was an aluminum metal with the diameter of 60 mm. Different thicknesses of Al_2O_3 were deposited at direct current power of 40 W under 1.3 Pa working pressure of the mixture of Ar and O_2. The thicknesses of Al_2O_3 were estimated by different sputtering time. The deposition rate of Al_2O_3 was about 3 nm min^{-1}. To ensure fair comparison, TiO_2 film was cut into two identical pieces. One was used to deposit Al_2O_3 and the other served as a reference.

2.3. Fabrication of DSSCs and measurements

A platinized conducting glass was used as a counter-electrode and 0.1 M LiI, 0.05 M I_2, 0.6 M 1,2-dimethyl-3-*n*-propylimidazolium and 0.5 M 4-*tert*-butypyridine in propylene carbonate was used as electrolyte. Both TiO_2 and TiO_2/Al_2O_3 electrodes were dipped in a N719 solution (0.5 mM in dry ethanol solution) for 12 h. The thicknesses of films were measured with a TalyForm S4C-3D profilometer (U.K.). The XPS measurements were carried out with a Thermo VG Multilab 2000 electron spectrometer (Thermo Electron Corporation) fitted with an Mg X-ray source. The surface morphologies of electrodes were observed by scanning electron microscopy (SEM, Sirion FEG, USA). The transmission and UV–vis absorption spectra were recorded on a UV–vis–NIR spectrophotometer (Cary 5000, Varian). The current–voltage (*I*–*V*) characteristics and dark current curves were measured using a 1000 W xenon lamp (Newport, USA) and a 2400 source meter (Keithley, USA), in which light intensity of 50 mW cm^{-2} was calibrated by a Si photodiode. The active area of the cells was 0.45 cm^2.

Cyclic voltammetry (CV) measurements were performed on a computer-controlled electrochemical workstation (CHI660A, CH Instruments, Inc., USA) in combination with a conventional three-electrode. The TiO_2 and TiO_2/Al_2O_3 (geometric surface area 1 cm^2) were employed as the working electrode. A Pt wire and a saturated calomel electrode (SCE) were used as counter electrode and reference electrode, respectively. In order to detect the interfacial electron transfer related reaction in the anodic TiO_2/electrolyte, CV was performed at a potential ranging from −1.2 to 0.6 V versus SCE in 0.2 M $LiClO_4$/PC solution (pH 2) at a scan rate of 100 mV s^{-1}. Impedance measurements were performed with a computer-controlled potentiostat (EG&G, BES). The frequency range is 0.01–100 kHz, and the magnitude of the modulation signal is 10 mV.

3. Results and discussion

3.1. Characterization of TiO_2/Al_2O_3

The thin TiO_2 films were used to deposit sputtered Al_2O_3, as described in Section 2. Though 10–15 μm TiO_2 films usually can achieve higher conversion efficiencies, we employed only very thin TiO_2 films intending to enhance the effects of the O_2 plasma and sputtered Al_2O_3 on the performance of the DSSC. To verify the presence of Al_2O_3 on TiO_2, the XPS spectrum of TiO_2 sputtered Al_2O_3 for 30 min (TiO_2/Al_2O_3 30 min) were carried out. As shown in Fig. 1, the Al 2s, Al 2p, Ti 2p, Ti 3p, C 1s, O 1s can be observed easily. The peaks detected at 458.86 eV for Ti 2p3/2 and at 37.52 eV for Ti 3p were in close agreement with Ti 2p3/2 (458.75 eV) and Ti 3p (37.5 eV) of TiO_2 while the peak at 532.29 eV can be attributed to O 1s. Peaks assignable to Al 2s and Al 2p were detected at 122.8 and 78.99 eV, respectively. They are very close to the data for Al 2s (120.8 eV), Al 2p (77.3 eV) in Al_2O_3, confirming the formation of Al_2O_3 on TiO_2. The binding energies were calibrated by taking C 1s peak (284.64 eV) as reference. Fig. 2 shows SEM micrographs for bare TiO_2 and TiO_2/Al_2O_3 30 min. It can be observed that the TiO_2/Al_2O_3 30 min electrode is porous. From the analysis of SEM in Fig. 2, it can be inferred that the porosity for TiO_2/Al_2O_3 films is a little smaller than that of bare TiO_2.

3.2. Optical properties of TiO_2/Al_2O_3

The DSSCs were illuminated from FTO substrate side in working conditions, so it needs to think about the optical properties when

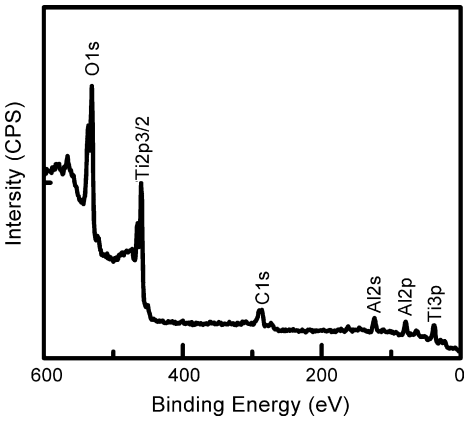

Fig. 1. XPS spectrum for TiO_2/Al_2O_3 30 min.

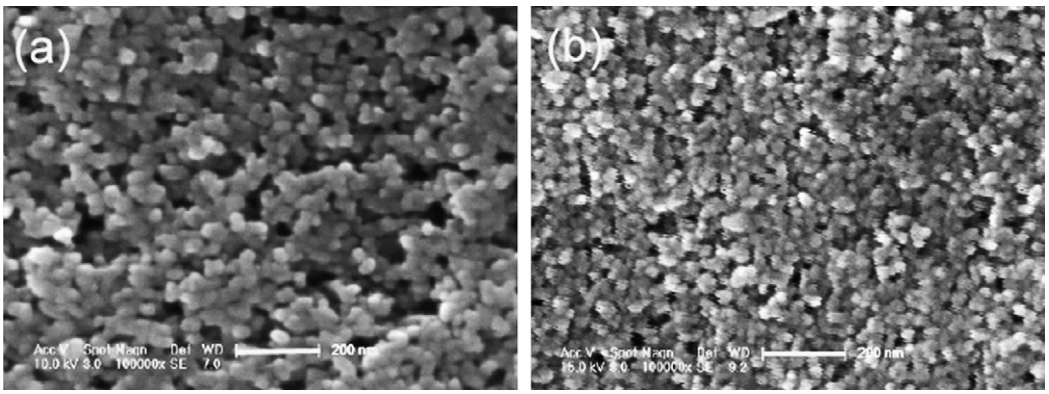

Fig. 2. SEM micrographs of bare TiO_2 and TiO_2/Al_2O_3 30 min: (a) bare TiO_2 and (b) TiO_2/Al_2O_3 30 min.

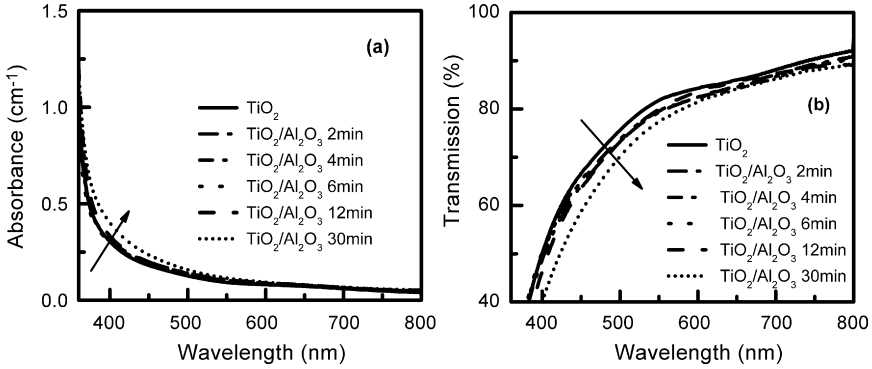

Fig. 3. Optical properties for TiO_2 and TiO_2/Al_2O_3 electrodes: (a) absorption spectra and (b) transmission spectra.

Al_2O_3 was sputtered on TiO_2. As shown in Fig. 3, the absorption and transmittance spectra change hardly when the sputtering time is less than 12 min, indicating that sputtering Al_2O_3 for less than 12 min does not influence the light absorption and transmission.

3.3. Dye absorption properties of TiO_2/Al_2O_3

Since Al_2O_3-coated surface is more basic than bare TiO_2, the higher basicity of TiO_2/Al_2O_3 surface favors dye attachment through its carboxylic acid groups. And in the process of the magnetron sputtering the O_2 and Ar plasmas create a hydrophilic surface which can cause the increase of adsorbed dye amount [19,20,28]. Therefore, an increase in dye adsorption is expected. Fig. 4 shows the UV–vis adsorption spectra for the dye-absorbed TiO_2 and TiO_2/Al_2O_3 electrodes. As expected, the metal-to-ligand charge-transfer (MLCT) absorption peaks significantly increased upon sputtering Al_2O_3 on TiO_2. It indicated that the dye adsorption is apparently enhanced with increasing sputtering time [3]. The increased dye absorption leads to enhanced light harvesting and thereby increased short-circuit photocurrent (J_{sc}) for the corresponding DSSCs. At the same time, it should be noted that the maximum absorption peak for N719, which is assigned to the MLCT band, blue shifts gradually with increasing sputtering time. The blue shift was attributed to the increased surface basicity due to Al_2O_3 modification. Upon Al_2O_3 coating, the coordination of Ti^{4+} to the carboxylates on the N719 dye is strengthened, thus resulting in the decrease in the electron density at Ru (α) center. The decrease in the electron density will stabilize the t_{2g} orbital and induce blue shifts of MLCT bands [4].

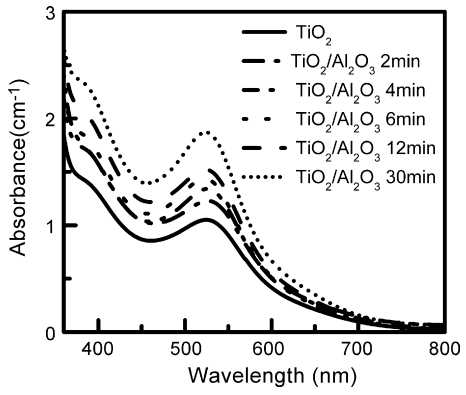

Fig. 4. UV–vis absorption spectra for N719-loaded TiO_2 and TiO_2/Al_2O_3 electrodes.

3.4. Comparison of current–voltage curves of TiO_2 and TiO_2/Al_2O_3 cells

Fig. 5 shows *I–V* curves for TiO_2 and TiO_2/Al_2O_3 cells in the dark and under illumination with the light intensity of 50 mW cm^{-2}. The corresponding solar cell parameters are summarized in Table 1.

Table 1
DSSCs performance of TiO_2 (N719) and TiO_2/Al_2O_3 (N719) electrodes under the light intensity of 50 mW cm^{-2}

Electrode	J_{sc} (mA/cm^2)	V_{oc} (mV)	FF	η (%)
TiO_2	4.27	668	0.689	3.93
TiO_2/Al_2O_3 2 min	4.49	674	0.711	4.30
TiO_2/Al_2O_3 4 min	5.97	691	0.716	5.91
TiO_2/Al_2O_3 6 min	3.95	716	0.713	4.03
TiO_2/Al_2O_3 12 min	3.25	640	0.671	2.79
TiO_2/Al_2O_3 30 min	1.61	607	0.617	1.21

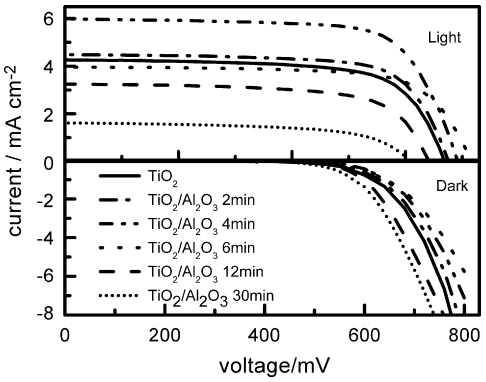

Fig. 5. *I–V* curves for TiO_2 and TiO_2/Al_2O_3 cells in the dark and under illumination with the light intensity of 50 mW/cm^2.

After sputtering Al_2O_3 for less than 4 min on TiO_2, the electrodes give higher short-circuit photocurrent (J_{sc}), open-circuit photovoltage (V_{oc}) and fill factor (FF). Especially in the case of TiO_2/Al_2O_3 4 min, the cell shows the great improvement in all cell parameters. The J_{sc} increases from 4.27 to 5.97 mA cm^{-2}, the V_{oc} from 668 to 691 mV, and the FF from 0.689 to 0.716. As a result, the cell efficiency (η) of TiO_2/Al_2O_3 4 min increases from 3.93% to 5.91%. It shows the positive roles of O_2 plasma treatment and Al_2O_3 coating on TiO_2. The increase of J_{sc} is consistent with the increased dye adsorption amount. With increasing sputtering time to 6 min, the V_{oc} further increases but J_{sc} decreases greatly, resulting in the decreased overall efficiency. Upon further increasing sputtering time, due to the drastic drop of all parameters, the DSSCs give poor conversion efficiency. The poor performances based on TiO_2/Al_2O_3 12 min and TiO_2/Al_2O_3 30 min revealed that excessive Al_2O_3 beyond tunneling distance would play a negative role in the photoelectron conversion process [16,27].

The dark current was not a good simulation of the recombination current under illumination. However, it can be used as an estimate of the extent of reduction of I_3^- with conduction band electrons. The dark current data in Fig. 5 shows that the dark current reduces gradually with increasing sputtering time for the first 6 min, indicating charge recombination between injected electrons and I_3^- ions being retarded in the procedure. The reduced dark currents account partly for the increased V_{oc} in TiO_2/Al_2O_3. On the basis of these results, it can be seen that the cells' performance is so sensitive that we need to control appropriate sputtering time in the DSSCs. And more detailed electrochemical analyses were carried out to understand the properties of TiO_2/Al_2O_3 electrodes prepared by the sputtering method.

3.5. Electrochemical characterizations

To demonstrate the effects of surface states on TiO_2 and TiO_2/Al_2O_3 electrode, cyclic voltammetry was conducted. Fig. 6 shows the typical CV curves of TiO_2 and TiO_2/Al_2O_3 in 0.2 M $LiClO_4$ solution. As shown in Fig. 6, scanning the bare TiO_2 and TiO_2/Al_2O_3 electrode potential in the negative direction yields a large featureless cathodic current. Scan reversal, however, yields an anodic current, which suggest that electron charging/discharge occurred at the anodic TiO_2/electrolyte interface, indicating Faradic currents in the electrolyte. In principle, for a perfect n-type semiconductor–electrolyte junction, charge injection will commence once the quasi-Fermi level reaches the lower edge of the conduction band. However, due to the presence of coordinatively unsaturated Ti species on the surface of TiO_2, some electronic levels exist at energies below the conduction band edge [29–31]. In the case of bare TiO_2 electrode, the anodic current starts to flow at −0.19 V versus SCE, whereas in TiO_2/Al_2O_3 4 min and TiO_2/Al_2O_3 30 min, the current starts to flow at a lower potential (−0.24 and −0.33 V versus SCE, respectively), as compared with the bare TiO_2. The modified TiO_2 surfaces induce shifts to a more negative potential region at the start point of the cathodic current. These indicated that the edge of conduction band of modified TiO_2 moves negatively toward the vacuum level. The phenomenon was due to better surface passivation on the surface of the anodic TiO_2 [31]. This demonstrated that the O_2 plasma treatment and Al_2O_3 coating passivate the surface states on TiO_2, resulting in a decrease in trap sites [32]. TiO_2 nanocrystals are not fully covered by dye molecules, and consequently, there are some surface areas directly in contact with the electrolyte. The use of the O_2 plasma treatment and Al_2O_3 coating passivate these surface areas, which makes a large contribution to the increase of J_{sc} and V_{oc} and is beneficial for the improvement on the performance of the DSSCs.

Electrochemical impedance spectroscopy (EIS) technique had been widely employed to study the kinetics of electrochemical and photoelectrochemical processes occurring in DSSCs [33–39]. We also investigated the effect of the O_2 plasma treatment and Al_2O_3 coating on the interface and kinetics in TiO_2 and TiO_2/Al_2O_3 cells by EIS technique. Fig. 7 shows typical electrochemical impedance spectra of TiO_2, and TiO_2/Al_2O_3 cells measured under forward bias (−0.8 V) in the dark. Responses in the frequency regions 10^3 to 10^5, 1–10^3, and 0.01–1 Hz were assigned to charge-transfer processes occurring at the Pt/electrolyte interface and TiO_2/dye/electrolyte interface, in Nernst diffusion within the electrolyte, respectively [40]. In the dark, the DSSC behaves as a leaking capacitor [41,42]. Under forward bias in the dark, electrons are transported through the TiO_2 network and react with I_3^-. At the same time, I^- is oxidized to I_3^- at the counter electrode. The dark reaction impedance due to electron transfer from the conduction band of TiO_2 to triiodide ions in the electrolyte is presented by the semicircle in intermediate frequency regime in the Nyquist plots [33]. The bigger the middle frequency semicircle in the Nyquist plots is, the slighter the electron recombination at the TiO_2/dye/electrolyte interface is.

It is clear to see that after the modification of TiO_2 by the sputtered Al_2O_3, the radius of the middle frequency semicircles in the Nyquist plot increase. The increase in the radius of the middle frequency semicircle in the Nyquist plot reveals the reduced electron recombination at the TiO_2/dye/electrolyte interface which is caused by the conduction band electrons of TiO_2 electrode captured by the reduction of I_3^- ions. The slightly increased resistance in TiO_2/Al_2O_3 4 min indicated that the coating of sputtered Al_2O_3 increases the surface resistance of TiO_2 electrode,

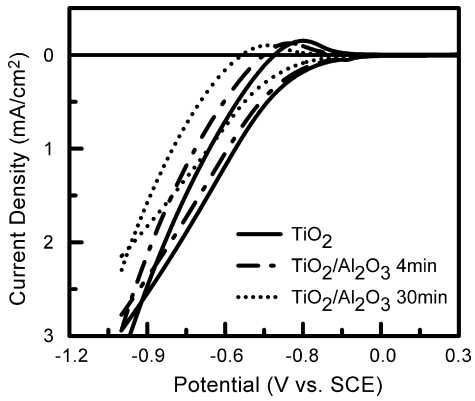

Fig. 6. Cyclic voltammograms of TiO_2 and TiO_2/Al_2O_3 electrodes in the 0.2 M $LiClO_4$/PC solution (pH 2). The scan direction with a scan rate of 100 mV/s is negative to positive potential. The active area is approximately 1 cm^2.

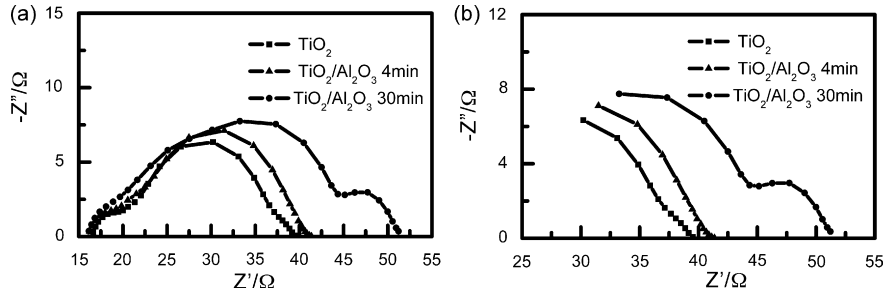

Fig. 7. (a) Impedance spectra for TiO_2 and TiO_2/Al_2O_3 cells measured at −0.8 V in the dark. (b) Magnified impedance spectra for TiO_2 and TiO_2/Al_2O_3 cells in low frequency range.

suppresses the back transfer of photo-generated electrons from TiO_2/Al_2O_3 4 min to the electrolyte, and reduce recombination at the TiO_2/dye/electrolyte interface. Therefore, the photo-generated electrons are extracted more efficiently, and thereby V_{oc}, FF, and J_{sc} increase together. However, excessive Al_2O_3 coating in TiO_2/Al_2O_3 30 min significantly increases surface resistance of TiO_2 electrode. Due to the increase of resistance, electron is difficult to transfer to the underlying SnO_2, resulting in the reduced electron injection and decreased conversion efficiency. It can be noted that the Nyquist plots consist of two semicircles in TiO_2 and TiO_2/Al_2O_3 4 min while it shows three semicircles in TiO_2/Al_2O_3 30 min. As shown in Fig. 7b, the semicircles for TiO_2 and TiO_2/Al_2O_3 4 min in the low frequency range are overlapped with that in the medium-frequency region. The semicircle for TiO_2/Al_2O_3 30 min occurs in the low frequency region corresponding to the larger Nernst diffusion within the electrolyte.

4. Conclusions

In summary, a novel surface modification method based on Al_2O_3-coated TiO_2 electrode was successfully developed by reactive dc magnetron sputtering in DSSCs. The study results show that the TiO_2 electrode sputtered Al_2O_3 for 4 min indicates the classic performance, which increases all cell parameters, resulting in improving efficiency from 3.93% to 5.91%. Further, with the increase of sputtering time, the conversion efficiency is decreased caused by the reduced electron injection efficiency. Further investigations had been done to study the characteristics of the Al_2O_3-coated TiO_2 electrode by the sputtering method. It was found that the Al_2O_3 coating and the O_2 plasma treatment increase dye adsorption amount, decrease trap sites on TiO_2, and suppress the back transfer of photo-generated electrons from Al_2O_3-coated TiO_2 electrode to the electrolyte at the TiO_2/dye/electrolyte interface. These findings open a way for using dc magnetron sputtering to fabricate an electronic insulating substance as a coating material in DSSCs.

Acknowledgements

We acknowledge the financial support of the Ministry of Science and Technology of China through Hi-Tech plan (No. 2006AA03Z347), and the help of the Nanoscience and Nanotechnology Centre and the Electron Microscope Centre at Wuhan University for the DSSC characterizations and measurements.

References

[1] B. O'Regan, M. Grätzel, Nature 353 (1991) 737–740.
[2] E. Palmares, J.N. Clifford, S.A. Haque, T. Lutz, J.R. Durrant, Chem. Commun. (2002) 1464–1465.
[3] Z.-S. Wang, M. Yanagida, K. Sayama, H. Sugihara, Chem. Mater. 18 (2006) 2912–2916.
[4] X. Wu, L. Wang, F. Luo, B. Ma, C. Zhan, Y. Qiu, J. Phys. Chem. C 111 (2007) 8075–8079.
[5] Z.-S. Wang, C.H. Huang, Y.Y. Huang, Y.J. Hou, P.H. Xie, B.W. Zhang, H.M. Cheng, Chem. Mater. 13 (2001) 678–682.
[6] S. Chappel, S. Chen, A. Zaban, Langmuir 18 (2002) 3336–3342.
[7] S.M. Yang, Y.Y. Huang, C.H. Huang, X.S. Zhao, Chem. Mater. 14 (2002) 1500–1504.
[8] S.G. Chen, S. Chappel, Y. Diamant, A. Zaban, Chem. Mater. 13 (2001) 4629–4634.
[9] E. Palomares, J.N. Clifford, S.A. Haque, T. Lutz, J.R. Durrant, J. Am. Chem. Soc. 125 (2003) 475–482.
[10] Y.S. Diamant, S.G. Chen, O. Melamed, A. Zaban, J. Phys. Chem. B 107 (2003) 1977–1981.
[11] S.J. Roh, R.S. Mane, S.K. Min, W.J. Lee, C.D. Lokhande, S.H. Han, Appl. Phys. Lett. 89 (2006) 253512–253514.
[12] K.-S. Ahn, M.S. Kang, J.K. Lee, B.C. Shin, J.W. Lee, Appl. Phys. Lett. 89 (2006) 013103–013105.
[13] M. Nanu, J. Schoonman, A. Goossens, Adv. Mater. 16 (2004) 453–456.
[14] J.H. Yun, S. Nakade, D. Kim, S. Yanagida, J. Phys. Chem. B 110 (2006) 3215–3219.
[15] H. Alarcon, M. Hedlund, E.M.J. Johansson, H. Rensmo, A. Hagfeldt, G. Boschloo, J. Phys. Chem. C 111 (2007) 13267–13274.
[16] A. Kay, M. Grätzel, Chem. Mater. 14 (2002) 2930–2935.
[17] H. Alarcon, G. Boschloo, P. Mendoza, J.L. Solis, A. Hagfeldt, J. Phys. Chem. B 109 (2005) 18483–18490.
[18] J.-B. Han, N. Wang, G.-P. Yu, Zh.-H. Wei, Zh.-G. Zhou, Q.Q. Wang, Sol. Energy Mater. Sol. Cell 88 (2005) 293–299.
[19] Y. Kim, C. Yoon, K. Kim, Y. Lee, J. Vac. Sci. Technol. A 25 (2007) 1219–1225.
[20] Y. Kim, B. Yoo, R. Vittal, Y. Lee, N.-G. Park, K.-J. Kim, J. Power Sources 175 (2008) 914–919.
[21] J. Weidmann, Th. Dittrich, E. Konstantinova, I. Lauermann, I. Uhlendorf, F. Koch, Sol. Energy Mater. Sol. Cells 56 (1999) 153–165.
[22] U. Diebold, J. Lehman, T. Mahmoud, M. Kuhn, G. Leonardelli, W. Hebenstreit, M. Schmid, P. Varga, Surf. Sci. 411 (1998) 137–153.
[23] J.-M. Pan, B.L. Maschhoff, U. Diebold, T.E. Madey, J. Vac. Sci. Technol. A 10 (1992) 2470–2476.
[24] B.-O. Aronsson, J. Lausmaa, B. Kasemo, J. Biomed. Mater. Res. 35 (1997) 49–73.
[25] S. Gan, Y. Liang, D.R. Baer, Surf. Sci. 459 (2000) L498–L502.
[26] J. Xia, N. Masaki, K. Jiang, S. Yanagida, Chem. Commun. (2007) 138–140.
[27] J. Xia, N. Masaki, K. Jiang, S. Yanagida, J. Phys. Chem. C 111 (2007) 8092–8097.
[28] J.-B. Han, X. Wang, N. Wang, Zh.-H. Wei, G.-P. Yu, Zh.-G. Zhou, Q.-Q. Wang, Surf. Coat. Technol. 200 (2006) 4876–4878.
[29] J. Moser, S. Punchihewa, P.P. Infelta, M. Grätzel, Langmuir 7 (1991) 3012–3018.
[30] A. Hagfeldt, M. Grätzel, Chem. Rev. 95 (1995) 49–68.
[31] Z.-P. Zhang, S.M. Zakeeruddin, B.C. O'Regan, R. Humphry-Baker, M. Grätzel, J. Phys. Chem. B 109 (2005) 21818–21824.
[32] S.H. Kang, J.-Y. Kim, Y. Kim, H.S. Kim, Y.-E. Sung, J. Phys. Chem. C 111 (2007) 9614–9623.
[33] Q. Wang, J.-E. Moser, M. Grätzel, J. Phys. Chem. B 109 (2005) 14945–14953.
[34] J. van de Lagemaat, N.-G. Park, A.J. Frank, J. Phys. Chem. B 104 (2000) 2044–2052.
[35] N. Papageorgiou, W.F. Maier, M. Grätzel, J. Electrochem. Soc. 144 (1997) 876–884.
[36] C. Longo, A.F. Nogueira, M.-A. De Paoli, H. Cachet, J. Phys. Chem. B 106 (2002) 5925–5930.
[37] L. Han, N. Koide, Y. Chiba, T. Mitate, Appl. Phys. Lett. 84 (2004) 2433–2435.
[38] Z.G. Chen, Y.-W. Tang, H. Yang, Y.-Y. Xia, F.-Y. Li, T. Yi, C.-H. Huang, J. Power Sources 171 (2007) 990–998.
[39] J. Xia, N. Masaki, K. Jiang, S. Yanagida, J. Photochem. Photobiol. A 188 (2007) 120–127.
[40] Z.-S. Wang, T. Yamaguchi, H. Sugihara, H. Arakawa, Langmuir 21 (2005) 4272–4276.
[41] Z.P. Huo, S.Y. Dai, K.J. Wang, F.T. Kong, C.N. Zhang, X. Pan, X.Q. Fang, Sol. Energy Mater. Sol. Cell. 91 (2007) 1959–1965.
[42] J. Bisquert, J. Phys. Chem. B 106 (2002) 325–333.